Development of Low-Order Regression Models for Selected Flat Spray Characteristics

K. M. Bade*, K. Cronce, R. J. Schick
Spray Analysis and Research Services, Spraying Systems Company, Wheaton IL 60187, USA
Kyle.Bade@Spray.com, Keith.Cronce@Spray.com, Rudi.Schick@Spray.com

Abstract

Dimensional as well as non-dimensional independent variables are used for predicting spray droplet size statistics and spray pattern distributions. The independent variables are: pressure, flow rate, spray angle, spray distance, viscosity, and surface tension. In the first approach, the dimensional values are used to develop a regression model for the general spray characteristics of interest; namely, Sauter mean diameter, spray width, and spray distribution profile shape. Secondly, a similitude approach is employed to generate dimensionless quantities from the independent variables, which are then used in formulating regression models. The similitude method allows for an assessment of the underlying balance of forces, which ultimately serve to form the spray characteristics. The final model development uses linear, or nonlinear where advantageous, regression models to fit the operational and rheological inputs to the spray characteristic outputs. The predictor models using dimensionless quantities showed a improved accuracy over the dimensional models. Additionally, the included number of dimensionless quantities is systematically reduced, revealing the most influential independent variables for each output. It is found that the Reynolds, Weber, and Froude Numbers are most influential. All models are developed for a particular nozzle, which limits the resulting models to this particular nozzle; however, the model *development process* has further reaching utility.

Introduction

In the spray nozzle and spray process design industry, it is advantageous to have a general idea of the spray characteristics for a nozzle in the beginning of the design stage, which can then be updated with more accurate testing results in the final design stages. To this end, the authors have engaged in an effort to develop low-order predictor models to provide these general spray characteristic using the results of detailed experimental testing. This type of model does not provide information regarding droplet breakup mechanisms, environmental conditions, or exact detailed spray characteristics; but does allow an accurate estimate of the spray characteristics over the defined input parameter range used to generate the models.

Previous efforts toward general spray characteristic estimators, have demonstrated reasonable accuaracy. The current study draws upon a very large experimental database in order to arrive at improved models while using new methods to improve the model predictions. The current study employs dimensionless quantities in an effort to generate more robust models. One previous study, Cronce, et.al. [1], demonstrated good agreement in the predicted distribution of spray profiles, but focused primarily on the combined profile overlap estimations and did not rigorously assess the accuaracy of the individual predicted spray distribution profiles. In an another study, Juslin et.al. [2] performed a regression analysis using three independent variables and an air-atomizing nozzle to assess the influence on each parameter on the resultant drop size. This study used an air-atomizing nozzle, motivated by the required atomization of a pharmaceutical spray application, which provides an atomizing-air parameter to primarily govern the drop size. Also, while an instructive and rigorous study, this effort did not investigate the spray width or distribution. While other spray characteristic regression model studies exist (see, for example, Solomon, et al. [7], Kirk [8], etc.), the majority of analysis has focused on drop size distribution alone, and to the author's knowledge, has never included the use of dimensionless quantities.

Experimental Methods

Experimental data was collected for thousands of nozzle operating parameter combinations in order to provide a database for the developed spray characteristic models. The collected data is for a specific type of nozzle and was collected using Laser Sheet Imaging and Laser Diffraction commercially available systems, which are described in relevant detail in this section.

The spray nozzle used in this experimental program, provided a flat-fan spray pattern. The modified Spraying Systems Co. TPU nozzle (PWMD tip) was a pressure driven (hydraulic) nozzle that allows for a wide range of spray angles, flow capacities. This nozzle was chosen in order to provide a flat-fan spray plume, which is generally tested in a patternation-table facility and is often employed in applications involving a target-on-conveyor

* Corresponding author: Kyle.Bade@spray.com

situation. Therefore, the spray pattern is most accurately assessed in a collapsed one-dimensional form. Readers are referred to [3] for further description of this nozzle type and a description of standard table Patternator testing practices.

Drop size measurements were acquired with a Sympatec Inc. HELOS-VARIO/KR Laser Diffraction (LD) system. The reader is referred to [4] and [5] for classic and current literature regarding the laser diffraction technique and the Sympatec implementation. In short, as droplets pass through a diffuse laser beam, a diffraction pattern is generated and the intensity distribution is measured by a 31-channel multi-element photo-detector array. This information is then processed for all detectable droplets and a drop size distribution is generated. Post-acquisition software, Windox 5, analysed the signals and accounted for any multi-droplet overlap in the data. For each distribution, statistical drop size measurements are calculated and reported. The Laser Diffraction instrument was setup with the TopMicron Module-R7 lens combination that allowed for a 0.5/18.0-3500um measureable drop size range using a 5mW HeNe laser with fibre optic transmission. To ensure accurate measurements, several setup considerations were employed including: an integrated auto setup system to provide auto-alignment, auto-focus, and auto-laser diameter adaptation; as well as positive-pressure purge-tubes to prevent lens wetting. The nozzle was setup on an overhead traverse with the major spray axis normal to the LD laser. The nozzle was then traversed in a quasi-steady manner so that the spray plume passed completely through the measurement domain at a constant nozzle to laser distance of 200mm. See Figure 1 for a schematic of this testing setup.

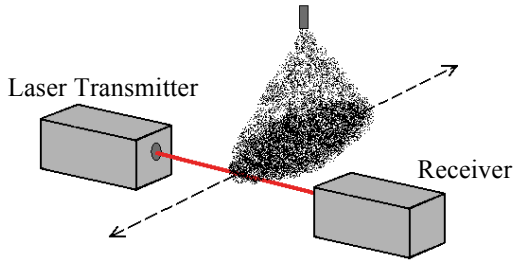

Figure 1 Laser Diffraction Testing Setup Schematic

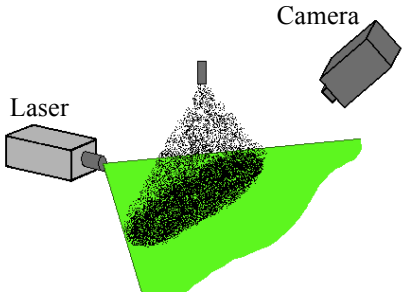

Figure 2 Laser Sheet Imaging Setup Schematic

Spray pattern distribution data were collected using a LaVision Laser Sheet Imaging (LSI) system. This system provided a time-efficient and high spatial-resolution method to characterize the planar spray coverage and distribution. In this setup, demonstrated in Figure 2, the LSI system was setup to measure normal to the spray axis over a wide spray-width range that was able to accommodate major axis widths in excess of the maximum, which was found to be 850mm. Laser sheet intensity correction was used to account for the non-uniform, Gaussian beam intensity variation across the laser sheet by acquiring multiple pre-test images using an oil-smoke generator to provide uniform drop seeding. An overhead traverse was used to change the spray distance to the laser sheet from 100-305mm, which was incorporated as an input parameter to the regression models. A minimum of 100 instantaneous images were acquired and ensemble averaged to generate a mean spray distribution at each combination of input parameters, with a pixel resolution of 0.583mm/pixel.

In the current experiments, Mie light scattering was used. These results are therefore inherently representative of the distributed sprayed droplet cumulative surface-area; however, preliminary experiments showed that these surface area distributions (Mie scattered light intensity) are adequately representative of volume distributions (Laser -nduced Fluorescence, LIF, light intensity) for these sprays. This is demonstrated in Figure 3; accordingly, the assumption will be made that the LSI data are representative of the average planar volume distribution. Furthermore, previous experiments [1] have confirmed LSI-LIF volume distributions to accurately match one-dimensional table patternation volume distribution results for these types of sprays. The two-dimensional LSI spray distributions were summed in the minor-axis direction (vertically in Figures 3a and 3b) to arrive at one-dimensional spray distributions to be used in the models, such as in Figure 3c.

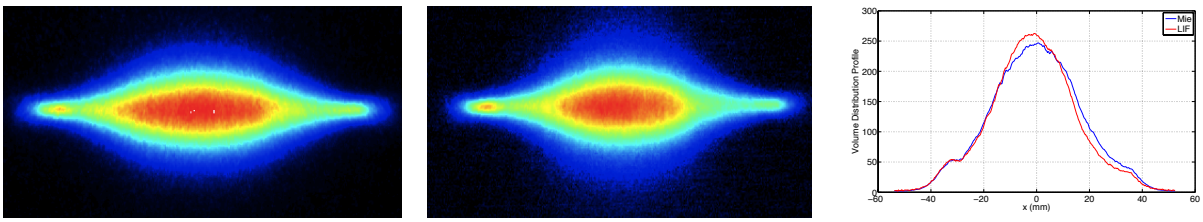

Figure 3 Two dimensional spray pattern distributions using (a) Mie and (b) Laser Induced Fluorescence, LIF, techniques. (c) Resultant one-dimensional spray pattern distributions, summed over the minor spray axis

Model development Methods

Two methods have been utilized in developing the regression models for the drop size and distribution profile data; namely, dimensional and a nondimension (similitude) approaches. In each case, a range of independent variables was investigated and will serve as the *input* parameters for the resultant *output* spray characteristic predictor models; Table 1 lists the dimensional parameters and the investigated ranges, note that the z-direction is in-line with the spray axis. For the drop size database, 1046 individual parameter combinations were tested; for the spray distribution database, 6002 independent variable combinations were collected. As noted in Table 1, regression models were developed for the entire database of experimental results, and also for a subset of data that only included the results using only water. Columns with a single value indicate a parameter held constant.

Table 1 Dimensional Independent Variable (input) Parameter Domain

Parameters		Drop Size Parameter Range				Distribution Parameter Range			
		All Data		Water Only		All Data		Water Only	
Pressure (bar)	P	1.38	20.7	1.38	20.7	1.38	20.7	1.38	20.7
Capacity (mL/min@2.76 bar)	c	9.5	113.6	9.5	113.6	9.5	113.6	9.5	113.6
Spray Angle (deg)	SA	65	110	65	110	65	110	65	110
z-Distance (mm)	z	203		203		100	305	100	305
Viscosity (Ns/m)	ν	0.001	0.15	0.001		0.001	0.15	0.001	
Surface Tension (N/m)	σ	0.03	0.0725	0.0725		0.029	0.0725	0.0725	
Density (kg/m^3)	ρ	998		998		998		998	

In order to develop a model for the one-dimensional spray distribution results that is scalable and yet low-order, a Fast Fourier Transform (FFT) technique was used to fit a trigonometric polynomial to each distribution profile. Equation 1 provides the FFT-fit equation form; note that the FFT sine component provides a solely imaginary contribution, and is therefore omitted. After detailed assessment of the raw and fit profiles, it was deemed adequate to use only the first seven FFT coefficients, n=0 to 6, thus reducing the order of the model (i.e. a reduced set of regression model fit parameters that corresponding to the FFT coefficients).

$$y(x) = a_0 + \sum_{1}^{\infty} a_n \cos(x) \tag{1a}$$

The reduced trigonometric polynomial fits are able to follow the raw one-dimensional profiles with an integrated profile volume difference to within 98.9% from that of the symmetric profiles. The agreement using the full set of FFT coefficients and reduced (first seven) coefficients was indistinguishable, this justifies using the reduced set of FFT coefficients with no significant loss in fit accuracy. Using the reduced order fit profiles allows predictor models to be generated for the FFT coefficients regardless of the profile width. This method effectively normalizes the volume distribution profiles using the only the lowest order FFT fit coefficients and provides consistency in the model development process.

In order to minimize error in the distribution profiles, the raw data profiles were mirrored about a calculated profile center point and averaged left-to-right, resulting in a symmetric profile for fitting. The process to determine the center point of each distribution profile was through a cross-correlation of each profile with its mirror image; the resultant correlation peak was deemed the center point. The symmetric profile was then created as an average of the left-and-right sides relative to this center point.

Finally, a trigonometric polynomial was fit to each symmetric profile, using the FFT-fit procedure described above. An arbitrary number of fit points were selected to provide an adequate capture of the variability of all profiles and visualize the results. For these efforts, the number of fit points was 25. A representative raw, symmetric, and fit profile are provided in Figure 4 as well as a histogram of the integrated profile volume difference between the symmetric and fit profiles to provide an indication of the error in the fits for all data profiles.

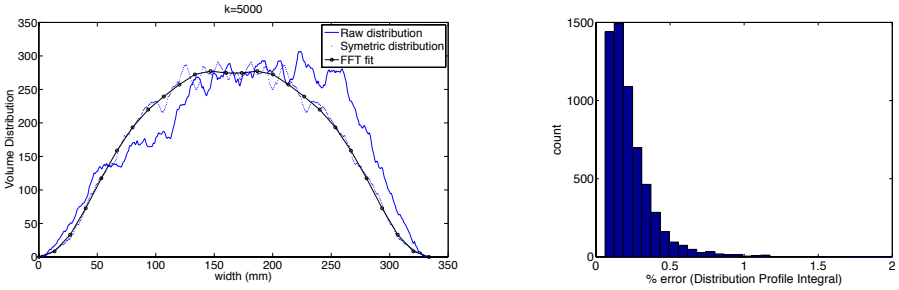

Figure 4 (a) Representative raw distribution profile, symmetric profile, and 25-point trigonometric polynomial (FFT) fit, (b) Histogram of profile volume-by-integration error between the symmetric and fit profiles

Similitude Analysis Approach

The independent dimensional variables are used to generate relevant dimensionless quantities in order to develop models that use relations of the independent variables rather than the input variables themselves to predict the spray characteristics. In doing so, an assessment of the relative importance of the dimensional variables may be conducted.

First, a set of *potentially* relevant dimensionless quantities was selected. These parameters are provided along with brief descriptions below describe the balance of forces inherent to each dimensionless parameter, see Equations 2-6 for definitions of these quantities.

$$\text{Reynolds Number} \propto \frac{\text{Inertial Forces}}{\text{Viscous Forces}} \qquad Re = \frac{\rho V L}{\sigma} \tag{2}$$

$$\text{Weber Number} \propto \frac{\text{Inertial Forces}}{\text{Surface Tension Forces}} \qquad We = \frac{\rho V^2 L}{\sigma} \tag{3}$$

$$\text{Ohnesorge Number} \propto \frac{\text{Viscous Forces}}{\sqrt{\text{Inertial} * \text{Surface Tension Forces}}} \qquad Oh = \frac{\mu}{\sqrt{\rho \sigma L}} = \frac{\sqrt{We}}{\text{Re}} \tag{4}$$

$$\text{Froude Number} \propto \frac{\text{Inertial Forces}}{\text{Gravitational Forces}} \qquad Fr = \frac{V}{\sqrt{gL}} \tag{5}$$

$$\text{Etros Number} \propto \frac{\text{Bouyancy Forces}}{\text{Surface Tension Forces}} \qquad Eo = \frac{(\rho - \rho_{air}) g L^2}{\sigma} \tag{6}$$

In Addition to the dimensionless quantities listed above, potentially relevant dimensional quantities were calculated and used in the development of some models. First, the nozzle rated capacity (i.e. flow rate at 40psi) which is dictated by the nozzle exit orifice area, was reduced to a characteristics length scale, C and used as the characteristics length scale, L. Next the spray distance and rated spray angle were used to calculate an idealized spray width, w_i. Finally, drag force was calculated using the capacity as the characteristic area and C_d=0.1.

$$\text{Exit Orifice Characteristic Length} \qquad C = \sqrt{\frac{capacity}{\pi}} \tag{7}$$

$$\text{Ideal Width} \qquad w_i = 2z\sqrt{\left[\sin\left(90 - \frac{spray\_angle}{2}\right)\right]^{-2} - 1} \tag{8}$$

$$\text{Drag Force} \qquad F_D = \frac{\rho_{air} V^2 A C_d}{2} \tag{9}$$

In the development of the final regression models, this set of dimensionless (and calculated dimensional) variables was reduced to only those that were determined to have a significant effect on the model outputs. The reduced models, using only those most important variables, are provided explicitly in the results section. Table 2 provides the data of Table 1 converted into relevant calculated dimensionless and dimensional values as described in Equations 2-9.

Table 2 Calculated and Dimensionless Independent Variable (input) Parameter Domain

Parameters		Drop Size Parameter Range				Distribution Parameter Range			
		All Data		Water Only		All Data		Water Only	
Reynolds Number (*10^8)	Re	0.00734	0.1356	0.3026	4.060	0.00416	0.1356	0.3026	4.060
Weber Number (*10^8)	We	0.4092	9.085	0.0723	3.759	0.2098	9.398	0.0723	3.759
Ohnesorge Number (*10^{-4})	Oh	14.00	193	0.4776	0.8880	0.0017	0.0187	0.4776	0.8880
Froude Number	We	3.167	15.06	2.239	16.14	2.239	16.14	2.239	16.14
Etros Number (*10^6)	We	0.5490	12.06	0.4160	4.992	0.0603	1.248	0.4160	4.992
Velocity	V	24.46	67.00	17.30	67.00	17.30	67.00	17.30	67.00
Capacity	C	2.018	6.083	1.756	6.083	6.083	6.083	1.756	6.083
Ideal Width	w_i	0.2589	0.5804	0.2589	0.5804	0.8712	0.8712	0.1295	0.8712
Drag Force (*10^4)	F_d	0.1391	3.131	0.0174	3.131	0.0689	3.131	0.0174	3.131

Regression Model Methods

In the regression model development, the independent variables were used in a regression model directly. The models were developed both for the dimensional parameters and non-dimensional parameters in order to find the optimal arrangement. Equations 10-14 were used in best-fit optimization schemes using the matlab function, *nlinfit*, to arrive at an optimal relationship between all parameters.

$$y(f_1 \ldots f_p) = r_0 + \sum_1^p r_p f_p \tag{10}$$

$$y(f_1 \ldots f_p, f_1 \ldots f_q) = r_0 + \sum_1^p r_p f_p + \sum_1^q r_q f_q^2 \tag{11}$$

$$y(f_1 \ldots f_p) = r_0 + \sum_1^p r_p f_p^2 \tag{12}$$

$$y(f_1 \ldots f_p, f_1 \ldots f_q) = r_0 + \sum_1^p r_p f_p + \sum_1^q r_q f_q^n \tag{13}$$

$$y(f_1 \ldots f_p) = r_0 + \sum_1^p r_p f_p^n \tag{14}$$

In equations 10-14, the p subscript indicates the number of independent parameters included in the regression model; additionally, all models included an offset parameter r_0. For models involving a linear (f^1) and nonlinear terms (f^2 or f^n), the q subscript indicates the second regression coefficient, where $p=q$ for all f. In all, there are $count(r_0+r_{\Sigma p}+r_{\Sigma q})=(1+\Sigma p+\Sigma q)$ regression coefficients for each model. The included parameters were then reduced in order to eliminate non-influential parameters without any significant loss in model accuracy; which indicated an insignificant correlation between any eliminated parameter and the output result.

Finally, an assessment of the most accurate regression models was conducted based on the mean and standard deviation of the model output parameters to the known spray characteristics with a preference given to the lower order linear models for simplicity. In the end, only regression models of the form of Equations 10 and 11 were found to be most accurate. This finding is significant in that higher-order models did not necessarily arrive at an increase in accuracy.

Results and Discussion

The results of the model development processes outlined above will first be used to explain the optimal model selection process for each modelled parameter (drop size, spray width, spray distribution), and then evaluate the specific accuracy of the *best* models. Each these modelled parameters will be shown for the dimensional and non-dimensional regression model cases for comparison; and also for a subset of input parameters which only includes the data for water as a spray material. These subset models are similar to the full models but with a fixed material viscosity and surface tension, often allowing for higher accuracy predictions.

Drop Size

For the purposes of this paper, a model for the Sauter Mean Diameter (D_{32}) drop size is developed. The model optimization was found to be similar across all drop size distribution statistical values. Figure 5 provides the results of the regression model (solid red line) for the dimensional and non-dimensional parameter inputs as well as an error histogram for each model. Additionally, dashed lines are provided in Figures 5a and 5b to show the 10% and 30% error ranges. The reduced order regression models used in the development of the results of Figure 5 are provided in Equations 15a and 15b and use the regression model form of Equation 10.

$$\begin{aligned} D_{32}(SA,Cap,Pres,Visc,SurfTen) = {} & (219) + (-0.495)SprayAngle + (0.464)Capacity \\ & + (-4.92)Pressure + (196)Viscosity + (-390)SurfaceTension \end{aligned} \tag{15a}$$

$$\begin{aligned} D_{32}(Re,We,Fr,Fd,Eo) = {} & (205) + (-3.85e-6)Re + (-8.72e-8)We \\ & + (-7.36)Fr + (-2.06e-4)Fd + (7.79e-6)Eo \end{aligned} \tag{15b}$$

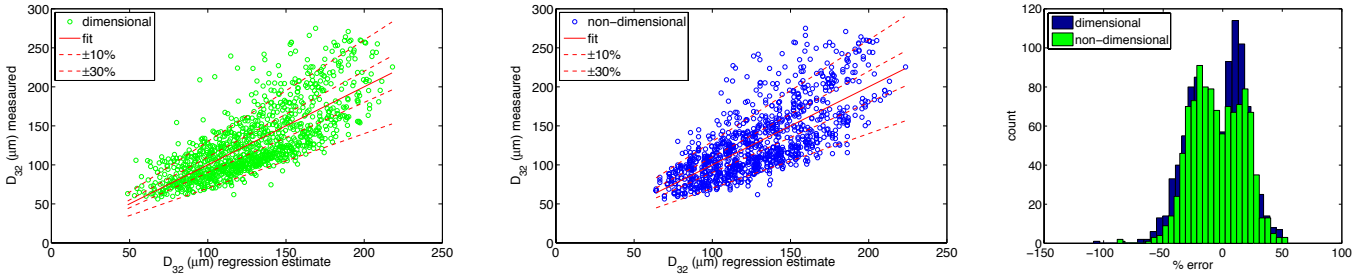

Figure 5 Linear regression model for D_{32} of various material rheologies, 1046 data points, using: (a) dimensional parameters (b) non-dimensional parameters and the (c) error histogram for each fit

The results demonstrated in Figure 5 show that a dimensionless parameter based model while similar in accuracy to the dimensional model, does provide an equivalently accurate model. Both models exhibit a double-peaked error histogram indicating that there is a dual-category separation in the accuracy of the models; it is not apparent what causes this divide. While no significant benefit to the dimensionless model is found here, the remainder of models outputs to exhibit a benefit and therefore this model will be selected as preferred. In Figure 5b, the regression model can be seen to provide a D_{32} prediction within 30% of the measured value for the vast majority of data points.

In an effort to develop a more accurate model for a subset of the Figure 5 data, a model was generated restricting the input data to that of water, which is the most often spray material for these nozzles. Figure 6 provides the results of this subset's regression model, using the same equations (eqn. 15a and 15b) but without any material rheology differences.

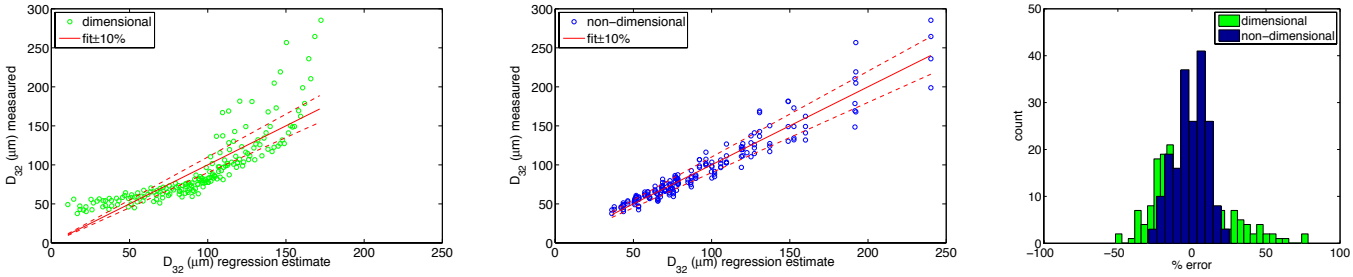

Figure 6 Linear regression model for D_{32} of the water, 189 data points, using: (a) dimensional parameters (b) non-dimensional parameters and the (c) error histogram for each fit

It is clear from Figure 6 that the model for the subset of water data has an improved result with the non-dimensional model and results in an accuracy error of approximately 10% or less. The regression model is provided in Equation 16, and the dimensionless parameters included in the model are shown.

$$D_{32}(\mathrm{Re},We,Fr,Fd,Eo) = (173) + (-1.51e-6)Re + (1.55e-6)We + (-8.00)Fr + (-0.007)Fd + (4.38e-5)Eo \quad (16)$$

Spray Width

The major-spray-axis spray width was modelled separately from the spray distribution profile shapes; this allowed for a normalized width distribution profile to be used in the FFT fits. Thus, the spray width was modelled in a manner similar to that of the drop size results. However, it was found that the non-dimensional model input parameters could be further reduced with no loss of accuracy. The fit equation for the dimensional model and dimensionless model followed the form of Equation 10 and are provided in Equations 17a and 17b.

$$w(SA,Cap,Pres,z,Visc,SurfTen) = (-472) + (5.73)SprayAngle + (-0.106)Capacity + (13.3)Pressure + (1.19)z + (194)Viscosity + (-1745)SurfaceTension \quad (17a)$$

$$w(w_i,Re,We,Fr) = (-135) + (704)w_i + (-2.85e-6)Re + (2.79e-7)We + (18.05)Fr \quad (17b)$$

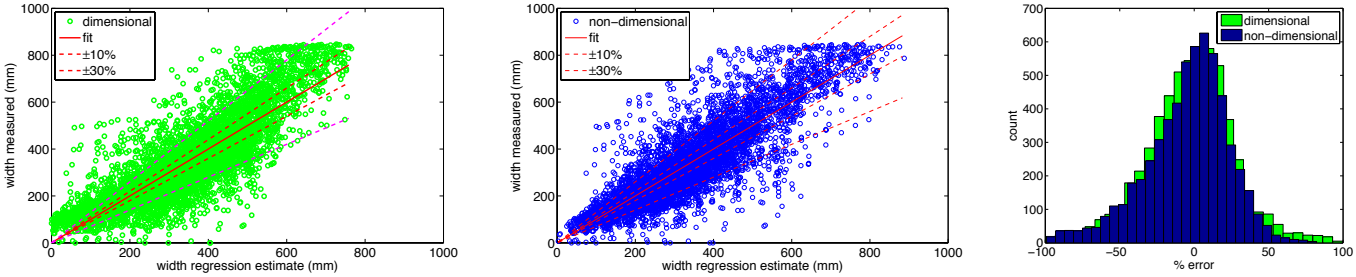

Figure 7 Linear regression model for spray width for a range of material rhelogies, 6002 data points, using: (a) dimensional parameters (b) non-dimensional parameters and the (c) error histogram for each fit

Figure 7 demonstrates the goodness of fit for the dimensional and non-dimensional regression models. More so than the drop size results, there is a clear benefit to the non-dimensional model, with the accuracy of the dimensionless model being within approximately within ±30% of the actual measured spray width, albeit with a notable portion of the estimated results still falling outside of the 30% intervals.

A reduced set of data containing only the results of the spray width for water was again generated and a subset regression model was developed. Equations 18a and 18b provide the regression model equations and Figures 8a and 8b demonstrate the goodness of fit for the dimensional and non-dimensional fit models. Clearly, the water models fit the data to within ±30% of the actual measured spray width; with an improvement over the more general models. Figure 8c shows the distribution of error form the measured and modelled subset of water-only data.

$$w(SA,Cap,Pres,z) = (-0.476) + (5.37e-3)SprayAngle + (-2.89e-4)Capacity + (0.0108)Pressure + (1.57e-3)z \quad (18a)$$

$$w(w_i,Re,We,Fr) = (-0.209) + (0.787)w_i + (1.36e-9)Re + (-1.20e-9)We + (0.0269)Fr \quad (18b)$$

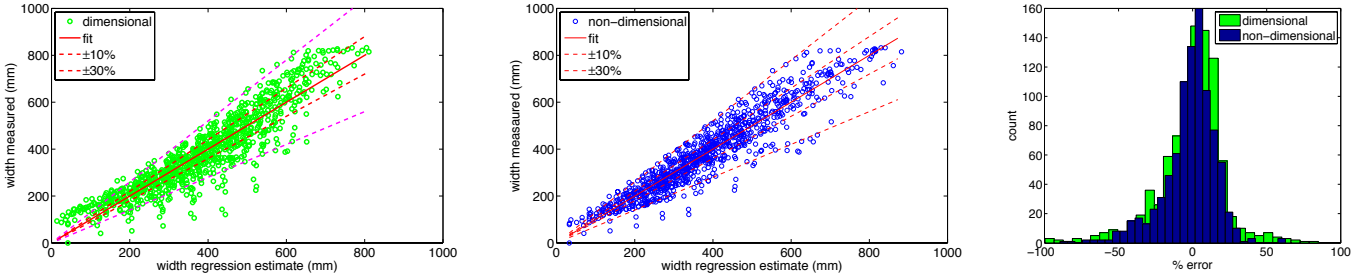

Figure 8 Linear regression model for spray width for water, 918 data points, using: (a) dimensional parameters (b) non-dimensional parameters and the (c) error histogram for each fit

As with the drop size regression models, the dimensional and non-dimensional models provide good model estimates with the dimensionless model providing a notably better accuracy. The dimensionless model has fewer large error data points, as demonstrated in Figure 8c, and is thus the *best* model result.

Spray Distribution

Finally, a regression model was developed for the first seven FFT coefficients for the symmetric fit profiles described in the *Model Developments Methods* section and demonstrated in Figures 4a and 4b.

In a similar manner to that described for the Sauter Mean Diameter and Spray Width results, a regression model was developed for each of the FFT coefficients. For brevity of this conference paper, each model (seven total for a_n, where n=0 to 6) is not explicitly shown here. However, Equations 19a and 19b demonstrate the final form used in formulating a best-case regression model for each case.

$$a_n(SA,Cap,Pres,z,Visc,SurfTen) = r_0 + (r_1)SprayAngle + (r_2)Capacity + (r_3)Pressure + (r_4)z + (r_5)Viscosity + (r_6)SurfaceTension \quad (19a)$$

$$a_n(Re,We) = (r_1)Re + (r_2)We + (r_3)Re^2 + (r_4)We^2 \quad (19b)$$

Notably, the dimensional model followed the form of Equation 10, as was the case for the Sauter Mean Diameter and Spray Width. However, the non-dimensional best-case regression model followed the second order form of Equation 11 with a reduced set of input variables, namely, only *Re* and *We*, and with no offset.

The results of the many spray distribution profiles, over six thousand total, do not lend themselves to be succinctly provided in detail, however, three representative profiles are provided in Figures 9a-c. Figure 9a represents a *good* model estimate result, Figure 9b represent a *somewhat bad* result, and Figure 9c represents a *bad* input profile leading to a bad model result.

The results in Figure 9a demonstrate a very accurate regression model results that shows the dimensional (purple) and non-dimensional (teal) profiles falling just below the target symmetric fit profile (black). The *bad* example of Figure 9b shows both models fall well below the fit-profile which closely matches the raw data profiles. As can be seen in Figure 9d, there were a fairly well distributed number of over- and under-estimated spray distribution profile results. Furthermore, Figure 9c demonstrates a common bad raw profile which exhibited a double-peak distribution profile, this is represented in the real spray by a "heavy-edges" spray pattern which is a non-desirable results. In future efforts, these types of profiles will be diagnosed and removed prior to final formulation of the regression model. This simple pre-model filtering of bad profiles will serve to remove many of the significant outliers in both the spray width and spray distribution error histograms.

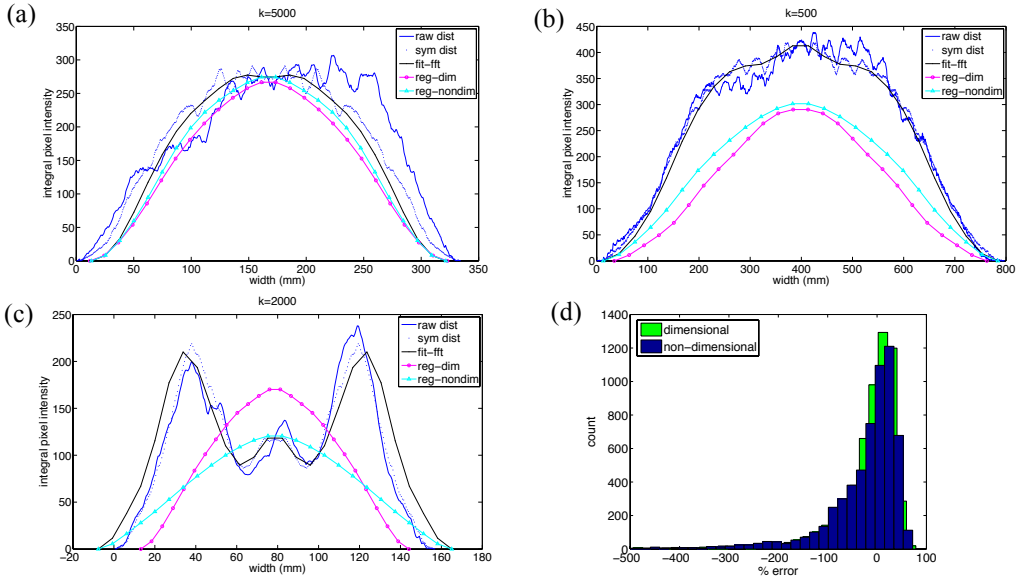

Figure 9 Representative spray distribution profile regression model results for (a) a good model results, (b) a bad model results, and (c) a bad input distribution result. (d) Histogram of the integrated volume error of each profile

Summary and Conclusions

The results of this work demonstrate the development of regression models to predict the spray drop size, spray width, and spray distribution over a range of independent input variables. The models are developed for dimensional and non-dimensional quantities and show an improvement in accuracy by using non-dimensional quantities. In either case, the results demonstrate predicted values to within approximately 30% or better of the measured values for the variable material data. This agreement increases to 10% for a regression models built from a subset of measured results using only water.

The optimal regression models have been shown to be of a *linear* regression model form for all cases except the model built for the non-dimension spray distribution profile data, which benefited from the addition of second order terms.

For future efforts, it is expected that the spray distribution profile predictions could be significant improved by removing distribution profiles with *heavy edges* as described in the results section, see Figure 9c. One possible solution may be to examine the fluctuation or rms of the distribution profile and then removing the high-rms profiles from the measured results database. Alternatively, an examination of the drop size results could provide an indication of poorly atomized sprays, which would then lead to a poor spray distribution and removal from the regression model input database.

Acknowledgements

The authors would like to thank Wojciech Kalata of Spraying Systems Co. for his past efforts on this project, as well as Stephen O'Donnell from Purdue University for his assistance in the collecting the large database of spray characteristics.

References

1. Cronce, K., Kalata, W., Schick, R.J., *Model to Predict Hydraulic Flat Spray Distribution*, ILASS Americas, 21st Annual Conference on Liquid Atomization and Spray Systems, Orlando, FL, May 2008.
2. Juslin, L., Antikainen, O., Merkku, P., Yliruusi, J., *Droplet size measurement: II. Effect of three independent variables on parameters describing the droplet size distribution from a pneumatic nozzle studied by multilinear stepwise regression analysis*, International Journal of Pharmaceuticals, Vol. 123. Pp. 257-264, 1995.
3. Spraying System Co., *Industrial Spray Products*, Catalog 70, pp.A5, pp.C21.
4. Sympatec HELOS VARIOS/KF Manual.
5. Heuer, M., Leschonski, K., *Results obtained with a new instrument for the measurement of particle size distributions form diffraction patterns*, Particle Characterization, Vol. 2, pp. 7-13, 1985.
6. LaVision SprayMaster Manual.
7. Solomon, K.H., Kincaid, D.C., Bezdek, J.C., *Drop Size Distributions for Irrigation Nozzles*, Transactions of the ASAE, Vol. 28(6), pp. 1966-1974, Nov.-Dec., 1985.
8. Kirk, I.W., *Measurement and Prediciton of Atomization Parameters from Fixed-Wing Aircraft Spray Nozzles*, Tansactions of the ASABE, Vol. 50(3), pp. 693-703, March, 2007.